The Force-Producing Mechanism for Centrosome Separation During Spindle Formation in Vertebrates Is Intrinsic to Each Aster

Jennifer C. Waters,* Richard W. Cole,* and Conly L. Rieder*‡

*Wadsworth Center for Laboratories and Research, Albany, New York 12201-0509; and ‡Department of Biomedical Sciences, State University of New York, Albany, New York 12222

Abstract. A popular hypothesis for centrosome separation during spindle formation and anaphase is that pushing forces are generated between interacting microtubules (MTs) of opposite polarity, derived from opposing centrosomes. However, this mechanism is not consistent with the observation that centrosomes in vertebrate cells continue to separate during prometaphase when their MT arrays no longer overlap (i.e., during anaphase-like prometaphase). To evaluate whether centrosome separation during prophase/prometaphase, anaphase-like prometaphase and anaphase is mediated by a common mechanism we compared their behavior in vivo at a high spatial and temporal resolution. We found that the two centrosomes possess a considerable degree of independence throughout all stages of separation, i.e., the direction and migration rate of one centrosome does not impart a predictable behavior to the other, and both exhibit frequent and rapid (4–6 μm/min) displacements toward random points within the cell including the other centrosome. The kinetic behavior of individual centrosomes as they separate to form the spindle is the same whether or not their MT arrays overlap. The characteristics examined include, e.g., total displacement per minute, the vectorial rate of motion toward and away from the other centrosome, the frequency of toward and away motion as well as motion not contributing to separation, and the rate contributed by each centrosome to the separation process. By contrast, when compared with prometaphase, anaphase centrosomes separated at significantly faster rates even though the average vectorial rate of motion away from the other centrosome was the same as in prophase/prometaphase. The difference in separation rates arises because anaphase centrosomes spend less time moving toward one another than in prophase/prometaphase, and at a significantly slower rate. From our data we conclude that the force for centrosome separation during vertebrate spindle formation is not produced by MT-MT interactions between opposing asters, i.e., that the mechanism is intrinsic to each aster. Our results also strongly support the contention that forces generated independently by each aster also contribute substantially to centrosome separation during anaphase, but that the process is modified by interactions between opposing astral MTs in the interzone.

THE equal distribution of chromosomes depends on spindle bipolarity which, in animal somatic cells, is established through the separation of replicated centrosomes. With few exceptions, the vertebrate centrosome consists of a mother and daughter centriole pair (i.e., a diplosome) and associated pericentriolar structures that nucleate many of the interphase cytoplasmic microtubules (MTs[1]; reviewed in references 9 and 36). In cycling cells, the centrosome is replicated near DNA synthesis (reviewed in reference 54) and then behaves as a single functional unit until the onset of mitosis (38).

As the cell enters mitosis, structural (e.g., 41) and chemical (e.g., 24, 53) changes occur in the centrosome and cytoplasm (e.g., 55) that lead to the resorption of cytoplasmic MTs and to the formation of centrosome-associated radial arrays of dynamically unstable MTs known as asters (reviewed in references 25 and 54). Spindle formation is then initiated as the centrosomes and their associated asters separate (reviewed in references 29 and 42). The exact timing of this separation, relative to nuclear envelope breakdown (NEB), varies considerably from cell to cell and can be initiated before or after the complete destruction of cytoplasmic MTs (6, 37, 38). After spindle formation, the centrosomes undergo an additional separation during anaphase when the spindle elongates.

Address correspondence and reprint requests to C. L. Rieder, Wadsworth Center for Laboratories and Research, P.O. Box 509, Albany, New York 12201-0509.

1. *Abbreviations used in this paper*: ALP, anaphase-like prometaphase; IMF, indirect immunofluorescence microscopy; LM, light microscopy; MTs, microtubules; NEB, nuclear envelope breakdown; NLC, newt lung cell; P/PM, prophase/prometaphase.

Whether centrosome separation during vertebrate spindle formation and anaphase occur by common or separate mechanisms is unclear. It is also unclear whether centrosome separation during these stages arises from a "push," e.g., as in the diatom from sliding interactions between adjacent and overlapping MTs derived from opposing centrosomes (e.g. 34, 37, 46, 50; reviewed in reference 22), from a "pull" generated independently by each centrosome (reviewed in references 1 and 31), or whether both mechanisms operate simultaneously (see reference 31).

In vertebrate cells the centrosomes most often initiate their separation during prophase before NEB. When this occurs, chromosomes closest to the centrosomes form an initial monopolar attachment at NEB, whereas those positioned equidistance between the centrosomes acquire a bipolar attachment and tether the asters (reviewed in reference 42). However, if the asters are far enough apart at NEB so that no one chromosome can acquire a bipolar attachment, an "anaphase-like prometaphase" (ALP; see references 8 and 40) mitotic figure is formed. In these cells, the two asters and their associated monooriented chromosomes continue to migrate apart in the absence of overlapping MT arrays (7, 44). Clearly, in these situations force-production for centrosome motion does not depend on MT–MT interactions between the asters.

Is the mechanism of centrosome separation during ALP, when their astral MT arrays no longer overlap, the same mechanism responsible for centrosome separation during prophase/prometaphase (P/PM) when their arrays overlap? Similarly, to what extent does this mechanism contribute to spindle elongation during anaphase B? A logical first step towards answering these and related questions is to determine whether the behavior and kinetics of separating P/PM centrosomes change once their arrays no longer overlap (as in ALP), and how this behavior compares to that of separating anaphase centrosomes. Unfortunately, because centrosome position is difficult to locate precisely in most living mitotic cells, a high-spatial and temporal-resolution analysis of their behavior during these three mitotic stages is lacking.

Here we show that the diplosome, which marks the position of each centrosome, is clearly visible by video light microscopy (LM) in living mitotic newt lung cells (NLCs). This feature has allowed us to compare the behavior of separating centrosomes at the time when their MT arrays overlap with that when they no longer overlap. Our data clearly reveals that force generation for centrosome separation during spindle formation in vertebrates is intrinsic to each aster, i.e., that the asters are pulled and not pushed apart.

Materials and Methods

Cell Culture

Primary newt (*Taricha granulosa*) lung cultures were grown in 0.5X L-15 media within Rose chambers as described by Rieder and Hard (43). When a suitable mitotic cell was located, the chamber was rapidly dismantled and the culture-containing coverslip mounted in a perfusion chamber for high resolution LM (see reference 17).

Indirect Immunofluorescence Microscopy

Cultures, some containing cells followed in vivo by LM, were fixed and processed for MT indirect immunofluorescence microscopy (IMF) as described by Rieder and Alexander (44). After the final wash, the chromosomes were stained with Hoechst 33342 (0.02 mg/mL) in PBS for 5 s. The cultures were then mounted on slides in PBS/glycerol (pH 7.8) containing *N*-propyl gallate. Cells processed for IMF were examined with a Nikon Optiphot microscope (Nikon Inc., Garden City, N.Y.) equipped with a 60X (NA = 1.4) phase-contrast objective. Double-exposure color images were recorded on Fujichrome Velvia (Fuji Photo Film Co., Tokyo, Japan), which was commercially processed.

Video Light Microscopy

Selected NLCs were observed in perfusion chambers at 20–22°C with a Nikon Microphot FX equipped with differential interference contrast (DIC) 60X (NA = 1.4) and 40X (NA = 0.85) objectives. Specimens were viewed with heat-filtered 480-nm light which was shuttered for time-lapse recording (see reference 4). Images were captured with a Hamamatsu C2400 video camera and simultaneously viewed on a monitor while routing to an Image-1 video processor (Universal Imaging Corp., Media, PA). Fixed noise and shading in the optical system were eliminated by background subtraction, and input images were averaged (16 frames) and contrast-manipulated in real time. After processing, each image was stored on a Panasonic TQ 2028 optical memory disk recorder (ADCO Aerospace, Ft. Lauderdale, FL). Framing rates were selected from 1.2 to 4.0 s.

Data Analysis

The particle tracking/analysis program within the Image-1 system was used to determine pixel changes in centrosome position between consecutive images. This system was calibrated in both the X and Y axes with a Nikon stage micrometer. This calibration was then verified by measuring the known (0.62 μm) frustule spacing of the diatom *Pleurosigma angulatum*. Total geometrical distortion in our system was calculated at ~4.8% between two perpendicular planes located in the central video field (see reference 4). Because geometrical decalibration was not performed, we minimized this error by routinely calibrating cursors in the plane of centrosome separation. Finally, contributions of stage drift and cell movement (which rarely occurs during mitosis) were estimated for each cell and found, in all cases, to be negligible.

For data analysis sequential video images recorded on optical memory disks were played back into the Image-1 processor through a time base corrector (For.A Corp, Natick, MA). For each frame both centriole pairs were located on a monitor and marked with a computer-generated cursor. The resulting pair of X and Y pixel coordinates was then recorded into the computer memory and imported directly into Quattro Pro 4.0 (Borland International, Inc., Scotts Valley, CA) for further manipulation and/or graphing.

Centrosome separation in vertebrates occurs slowly ($\leq$2 μm/min) during all stages of mitosis. Thus, when framing rates were >20 per min, frame-to-frame changes in centrosome position were subtle and difficult to determine on the monitor. To minimize this ambiguity we analyzed all of our sequences at 4-s intervals. Changes in the distance between centrosomes (*direct-distance graphs*) were calculated by determining the length of a line connecting the two diplosomes in each successive frame.

Determining the *relative contribution* that each centrosome makes to the separation process was less straightforward because the cells contained no stationary fiduciary markers, and both centrosomes exhibited motions that did not increase or decrease the distance between centrosomes. To estimate the individual contribution each makes to the separation process we used Eq. 1, which solves for S_1 and S_2 in Diagram 1.

As long as a was $\leq$10°, our equation provided a close approximation of those vectorial components of motion that were parallel to a line drawn between the previous position of the two diplosomes. Because our sampling rate was high (every 4 s), and centrosomes move slowly, a was never >4° in our study. The data obtained from Eq. 1 could be displayed as movement-per-frame bar graphs or relative-contribution distance/time plots (see Fig. 3, *D* and *E*). In these graphs, the movement of a centrosome from its previous position that increased the separation distance relative to the previous position of the other centrosome was considered "away" motion and recorded as positive. Similarly, movement of a centrosome from its previous position that decreased the relative separation distance was considered "toward" motion and recorded as negative. Eq. 1 does not discriminate between toward and away vectorial components produced when the whole spindle is shifted, for any reason, along the centrosome–centrosome axis. To eliminate this rare event we deleted both data points when the vectors from both centrosomes had the same magnitude but in opposing directions.

The validity of our approach for estimating the contribution that each centrosome makes to the separation process is confirmed by the fact that, for any one cell, the sum of the two centrosome contribution curves calcu-

$$S_1 = -(V_{O1O2} \cdot V_{N1N2})/\sqrt{[(X_{O2} - X_{O1})^2 + (Y_{O2} - Y_{O1})^2]}$$
$$S_2 = -(V_{O2N2} \cdot V_{O2O1})/\sqrt{[(x_{O2} - x_{O1})^2 + (Y_{O2} - Y_{O1})^2]}, \quad (1)$$

(where $\cdot$ = Dot product = $(X_{N1} - X_{O1}) * (X_{O2} - X_{O1}) + (Y_{N1} - Y_{O1}) * (Y_{O2} - Y_{O1})$ V = vector, and X,Y = coordinates of positions O and N.

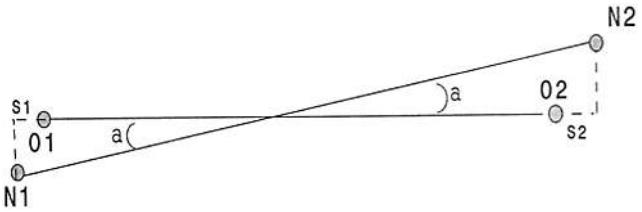

Diagram 1. O1 and *O2* are the positions of the centrosomes at time zero; *N1* and *N2* are the positions of the centrosomes at + 4 s; *O1* ---- *O2* is the distance between centrosomes at time zero; *N1* ---- *N2* is the distance between centrosomes at + 4 s. *a* is the angular change between the centrosome–centrosome axis at T = 0 and T = 4 s.

lated using Eq. 1 falls on the curve obtained from direct distance measurements (e.g., the summation of curves *1* and *2* on Fig. 3 *D* is indistinguishable from curve *3*).

The relative-contribution analyses do not portray the randomly directed displacements of each centrosome, clearly evident on our time-lapse recordings. These data can be most readily conveyed by two-dimensional *space-versus-time graphs*, in which changes in the X and Y coordinate of each centrosome are continuously plotted against time (because the centrosomes were co-planar throughout our periods of analyses, movement in the Z axis was considered negligible). Unfortunately, spatial confusion created when a centrosome moves back through one or more of its previous positions makes the plots progressively more difficult to interpret. In addition, the temporal aspect of the plots is rapidly degraded when one centrosome remains stationary while the other is moving because time cues cannot be inserted owing to space limitations. We minimized this spatial confusion by restricting our analyses to representative 4-min, 40-s (i.e., 70 frame) "windows." We also developed a novel approach for reducing temporal confusion that involved representing the positional changes incurred by each centrosome over the same 28-s period (seven frames) in the same color, and then varying the color between periods.

Two-sample *t* tests were used to compare the data between mitotic stages. Because there was no statistically significant difference over all of the parameters that we measured between separating centrosomes in P/PM and ALP cells, these data were pooled for comparison with anaphase centrosomes.

Results

The various routes of spindle formation in NLCs are diagrammed in Fig. 1, and the distribution of MTs during the stages germane to our study are shown in Fig. 2. In many NLC's, each centrosome could be clearly followed in vivo with differential interference contrast optics, and the diplosome could often be resolved with a 60× objective (inset in Fig. 3 *C*). During our study we found that the relative position of the mother and daughter centrioles comprising the diplosome remained fixed with respect to one another, and that rotational movements of the aster invariably induced a similar movement in the diplosome (data not shown).

Structural and Kinetic Analysis of Separating Centrosomes

Prophase/Prometaphase. The replicated centrosomes are first visible by anti-tubulin IMF in late prophase cells (Fig. 2 *A*). Separating centrosomes could not be clearly followed in living cells when the process was delayed until after NEB (pathway *A* in Fig. 1). Therefore, we selected cells in which the centrosomes initiated their separation well before NEB, which occurred in the majority of cases (pathway *B* in Fig. 1). In these cells, centrosomes began separating before complete disassembly of the interphase MTs (Fig. 2 *B*). During the initial separation stages, a weak aster was associated with each centrosome, while MT density between the asters was no greater, and often less, than expected from two overlapping arrays (Fig. 2 *B*). By NEB, the great majority of MTs were associated with the asters (Fig. 2 *C*).

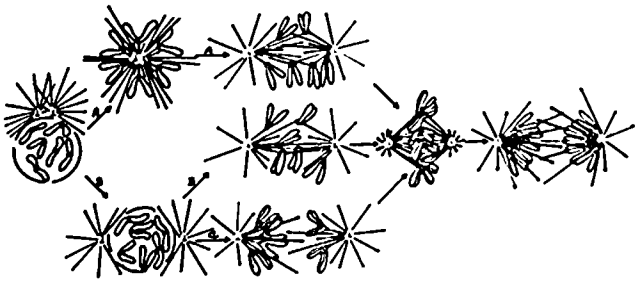

Figure 1. Schematic diagram outlining the different pathways of spindle formation in NLC's. Spindle formation proceeds along the upper pathway (route *A*) if NEB occurs before centrosome separation and along the lower pathway (route *B*) if NEB occurs during or shortly after centrosome separation. Anaphase-like prometaphase (route *C*) is a derivation of the lower pathway. See text for details.

The aster often radially arrayed particles and mitochondria. When this occurred we could locate the replicated but unseparated centrosome in living late prophase cells. However, we were unable to clearly visualize the initial splitting of the diplosomes due to the accumulation of organelles near the aster center, and the lack of detectable clues indicating that the process was under way. The diplosomes could be clearly seen as individuals only after their associated asters had migrated a sufficient distance apart (~5–8 μm) to be detectable as two independent arrays (Fig. 3 *A*).

Distance changes between the centrosomes could be determined from direct-distance curves, which plot at various time intervals the length of the line connecting them (Fig. 3 *D*, curve *3*). However, in every cell centrosome separation was characterized by periods in which each centrosome exhibited no motion, followed by periods in which each moved at unpredictable angles relative to the previous centrosome–centrosome axis. (Fully separated centrosomes in prometaphase/metaphase cells also exhibited independent, and sometimes exaggerated, motions that were lateral to the previous centrosome-centrosome axis [data not shown]). During the separation process, motion in one centrosome was rarely linked to a similar but opposite-directed motion in the other (e.g., Fig. 4 *A*). As a result, the increase in distance between them was achieved via highly variable pathways. These findings are best documented on two-dimensional space-time plots (see Materials and Methods). These plots showed that centrosomes could undergo displacements of 4–5 μm/min and that some of these motions were at angles to the previous centrosome–centrosome axis (Fig. 4 *A*). The average distance moved by a centrosome in any set of directions was 2.16 (SEM) ± 0.23 μm/min (see Table I, line 1).

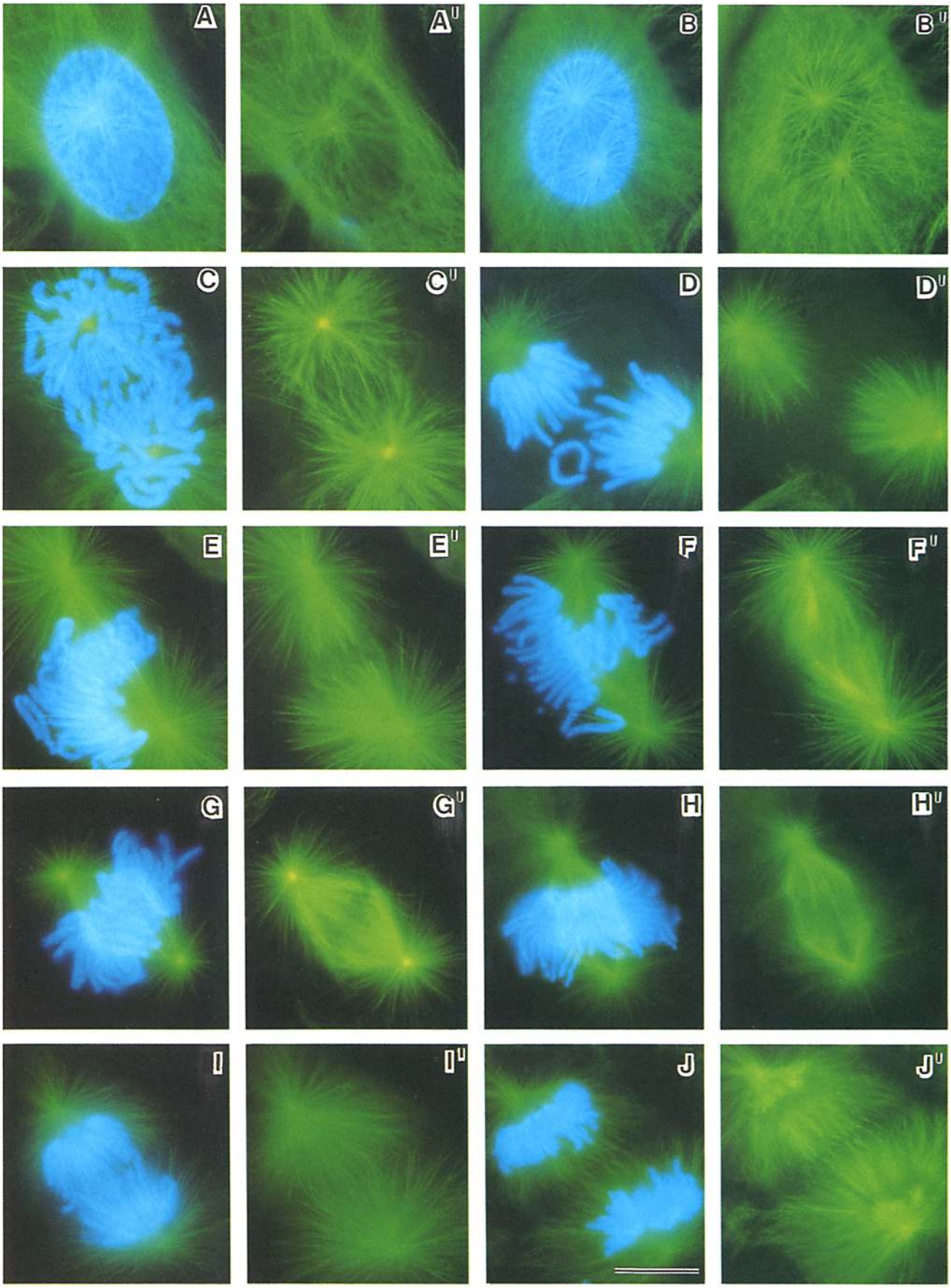
A
A'
B
B'
C
C'
D
D'
E
E'
F
F'
G
G'
H
H'
I
I'
J
J'

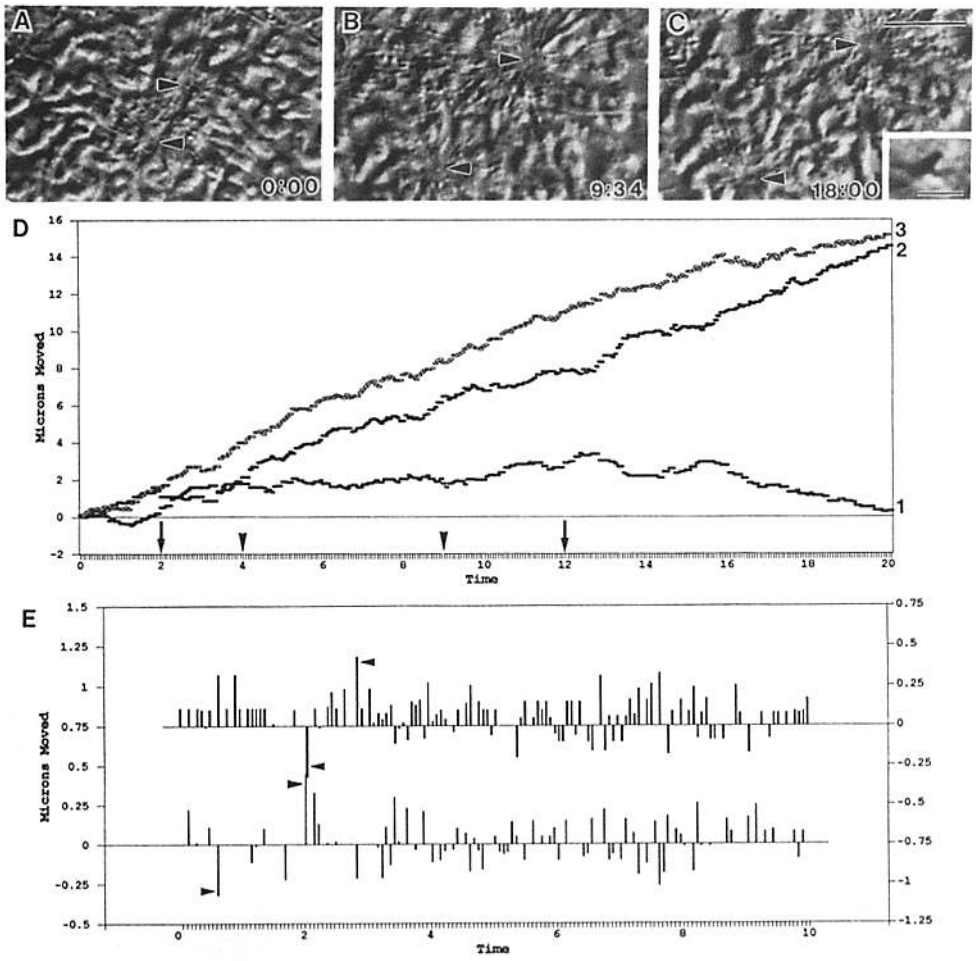

Figure 3. (*A–C*) Video micrographs of centrosomes (*arrowheads*) separating in a prophase cell. Time in min:s in lower right hand corner. The inset in *C* is from another cell in which the orthogonal mother/daughter centriole relationship is clearly visible. (*D*) Relative contribution (curves *1* and *2*) and direct distance (curve 3) plots for the separating centrosomes pictured in *A–C*. The separation distance (vertical axis) was normalized to 0 at the start of the analysis. Arrows along the time axis note the 10-min window analyzed in *E*, while the arrowheads note that time period covered by the two-dimensional space-time plot in Fig. 4 *A*. (*E*) Bar graph of data obtained from Eq. 1 (see Materials and Methods) for both centrosomes pictured in *A–C*. Between any 4-s time interval each centrosome could remain stationary or exhibit a vectorial component of motion toward (−) or away (+) from the other centrosome. Arrowheads note ± vectors that approach 6 μm/min. Bars (*C*) 10 μm; (inset) 0.5 μm.

There were periods when the centrosomes were undergoing little if any separation. Also, our filming durations differed considerably, depending on the cell or mitotic stage. Therefore, to more fairly compare data sets within and between mitotic stages, we selected for comprehensive analyses the 10-min window, from each direct-distance plot, in which the centrosomes underwent the greatest separation (e.g., *arrows* in Fig. 3 *D*). The following analyses were based on nine cells, followed for 10 to 33 min, in which the separating centrosomes were continuously visible before, during, and after NEB.

The traditional direct-distance plot (e.g., curve *3*, Fig. 3 *D*) provides no information on the relative contribution that each centrosome makes to the separation process. To obtain this information, we analyzed the input data from each 10-min window using Eq. 1 (see Materials and Methods), which allowed us to closely approximate, on a frame-by-frame basis, the vectorial component of each centrosome's motion that altered the distance between centrosomes. This, in turn, provided us with a number of analyzable characteristics that describe the separation process. For each centrosome, these data could be displayed as movement-per-frame bar graphs (Fig. 3 *E*) and relative-contribution distance/time plots (curves *1* and *2* in Fig. 3 *D*).

Like the two-dimensional space-time plots, the relative-contribution analyses revealed that within each framing interval one or both centrosomes could: (*a*) remain stationary or exhibit motion having no vectorial component that alters the centrosome–centrosome distance (hereafter termed "stationary"), (*b*) have a vectorial component of movement "away" from the other centrosome (positive motion on Fig. 3 *E*), or (*c*) have a vectorial component of motion directed "toward" the other centrosome (negative motion on Fig. 3 *E*; cf Figs. 3 *E*, and *4*). Approximately half the time each centrosome exhibited no movement or movement that did not change the distance between centrosomes (see Table I, line 2). However, when the motion of a centrosome affected the distance between centrosomes, it more frequently increased the separation distance (30%) rather than decreasing it (20%).

Figure 2. A gallery of fluorescent micrographs depicting the distribution of both chromosomes and microtubules (*A–J*), and microtubules alone (*A'–J'*), during spindle formation along pathways B and C in Fig. 1. (*A*) Duplicated but unseparated prophase centrosomes; (*B*) separating prophase centrosomes; (*C*) immediately after NEB with well separated centrosomes; (*D*) anaphase-like prometaphase (pathway C in Fig. 1); (*E*) early prometaphase (pathway B in Fig. 1); (*F*) late prometaphase; (*G*) metaphase; (*H*) early anaphase; (*I*) mid anaphase; (*J*) late anaphase. Bar (*J*), 20 μm.

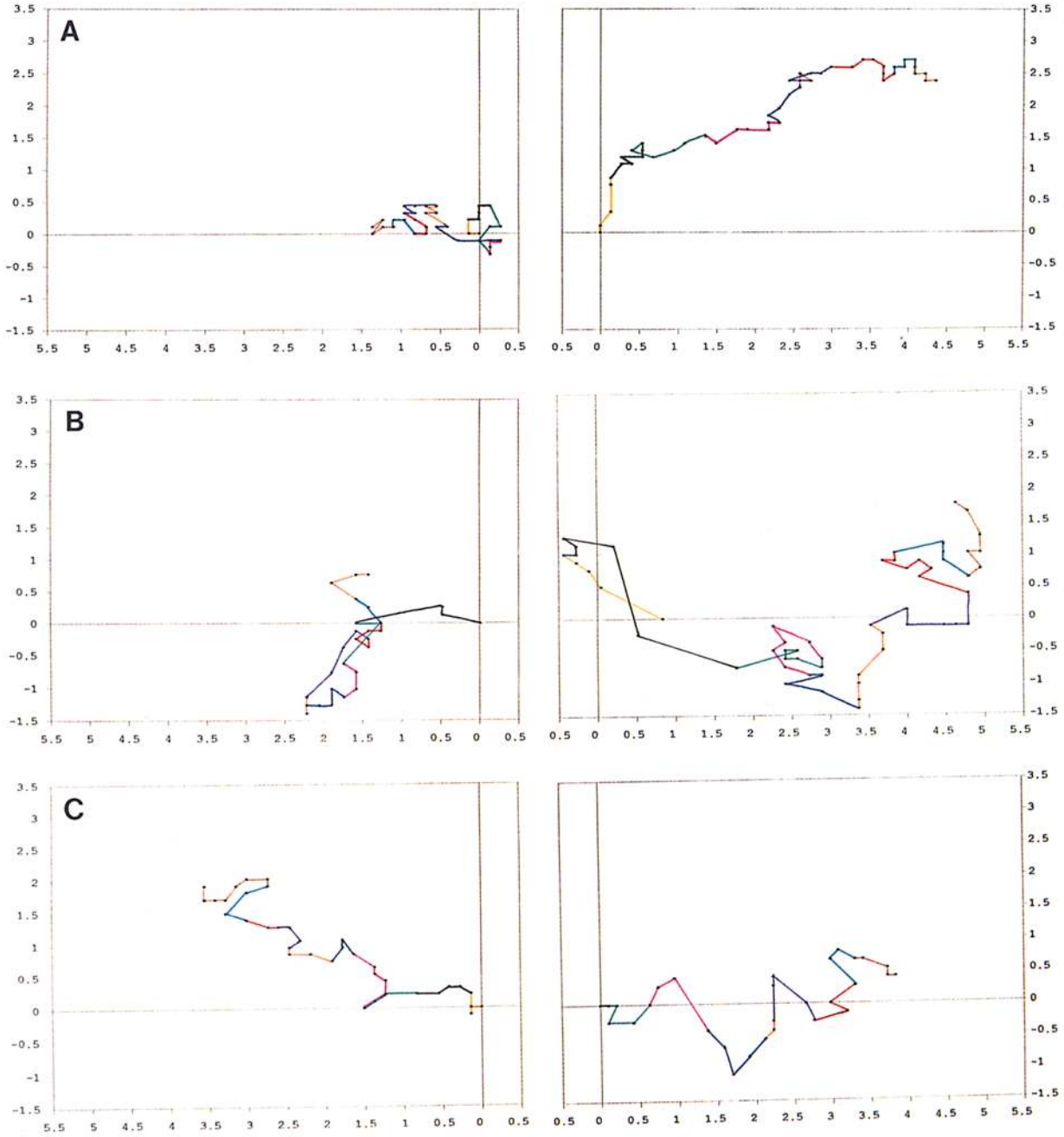

Figure 4. Two-dimensional space-time plots of the separating centrosomes in the prophase (*A*), ALP (*B*) and anaphase (*C*) cells shown in Figs. 3, 5, and 6, respectively. Each plot consists of left- (centrosome No. 1) and right- (centrosome No. 2) hand sides which together depict the displacement of both centrosomes during the same 4-min 40-s interval. The plot for each centrosome starts at the 0 intersect of the X and Y axes, and each is subdivided into ten consecutive color-coded segments. Each of these segments documents the X and Y motion, in micrometers, of that centrosome over seven 4-s frames. Matching colors in the left- and right-hand sides reflect the same time period. Colored segments containing less than seven data points, or missing segments, reflect that the centrosome was stationary for one or more time points. See text for details.

In these analyses, the greatest vector of motion observed for any one centrosome, toward or away from the other centrosome, was ~5–6 μm/min (*arrowheads* in Fig. 3 *E*). This compares favorably with the above noted maximum total displacement of centrosomes (~4–5 μm/min) determined from frame-by-frame changes in pixel coordinates.

Up to this point our results indicated that each separating centrosome possessed the ability to move independently in any direction. We therefore asked the question, when a centrosome exhibits toward or away motion, what is the average rate of this component? For each centrosome this figure was obtained by summing all of the toward and away vectorial components of motion during the 10-min window, then dividing by the number of (4-s) frames in which such motion was observed, and then multiplying by 15 to get μ/min. The average rate of the away vector was determined to be 0.80

Table I. Kinetic Characteristics of Separating Centrosomes

Type of Analysis	P/PM (N = 18*)	ALP (N = 14)	Anaphase (N = 14)
		$\chi \pm SEM$	
1. Average total displacement per min (μm)‡,§	2.16 ± 0.23	2.42 ± 0.28	2.18 ± 0.17
2. Frequency (percent) of:‡,‖			
no motion¶	47.4 ± 5.0	53.9 ± 7.4	48.1 ± 4.0
toward vector**	19.8 ± 3.0	18.2 ± 2.7	13.0 ± 1.6
away vector‡	32.9 ± 2.9	27.8 ± 4.9	38.9 ± 3.2
3. Average rate of away vector (μm/min)‡,‖,§§	0.80 ± 0.08	0.76 ± 0.12	0.86 ± 0.08
4. Average rate of toward vector (μm/min)‡,‖,‖‖	0.47 ± 0.09	0.46 ± 0.05	0.18 ± 0.02
5. Ratio of toward/away distance moved‡,‖,¶¶	0.54 ± 0.07	0.70 ± 0.08	0.28 ± 0.06
6. Average separation rate (μm/min) during most activity‡,‖	0.38 ± 0.07	0.30 ± 0.10	0.58 ± 0.08
7. Average separation rate (μm/min) during observational period‖	0.28 ± 0.06	0.24 ± 0.09	0.51 ± 0.07

* Number of centrosomes (= 2× the number of cells).
‡ 10-min window during which the two centrosomes exhibited the most separation.
§ Average distance moved by each centrosome, regardless of direction, as determined from frame-by-frame changes in pixel coordinates.
‖ The relative contribution each centrosome makes to the separation process. Includes only that vector of motion which increases or decreases the distance between centrosomes (determined from Eq. 1, see Materials and Methods).
¶ Percentage of frames in which centrosome position did not change, or the positional change did not increase or decrease the centrosome–centrosome distance.
** Percentage of frames that centrosome showed a vectorial component (→) of motion toward other centrosome.
‡‡ Percentage of frames that centrosome showed a vectorial component (→) of motion away from other centrosome.
§§ Only that vectorial component of each centrosomes motion contributing to an increase in the distance between centrosomes.
‖‖ Only that vectorial component of each centrosomes motion contributing to a decrease in the distance between centrosomes.
¶¶ Absolute value of total toward motion (summed in micrometers) divided by total away motion.

± 0.08 μm/min, whereas the average rate of the toward vector was 0.47 ± 0.09 μm/min (Table I, lines 3 and 4). These figures are significantly different by the two-sample t test (P = 0.01).

In addition to exhibiting a greater away than toward vector component, each centrosome also underwent a higher frequency of away motion. As a result, the average ratio of toward versus away distance moved over 10 min was <1 (0.54 ± 0.07; Table I, line 5)—an obvious prerequisite for separation. The average net rate contributed by each centrosome to the separation process was then calculated by summing all of the away vectorial components of motion, subtracting from it the absolute value of the summed toward components, and dividing by the time interval. On average, each centrosome exhibited a net away vectorial motion component of 0.38 ± 0.07 μm/min during the 10-min window of greatest separation (Table I, line 6). This was slightly higher than the average over the duration of separation (0.28 ± 0.06 μm/min; Table I, line 7).

In summary, as the centrosomes separate to form the spindle, each spends ~70% of the time "stationary" or exhibiting a vector of motion toward the other centrosome. When a centrosome does exhibit a vectorial component of motion away from the other centrosome, the average rate of this component is statistically greater than that exhibited when moving toward the other centrosome. However, in both cases these vectorial components represent only a fraction of the actual distance moved by the centrosome.

Anaphase-like Prometaphase. If the distance between the asters was 60 μm or more at NEB the two MT arrays exhibited little or no overlap (Fig. 2 *D*; see also reference 44). Under this condition, an ALP mitotic figure was commonly formed (pathway *C* in Fig. 1). In rectangular-shaped cells, the ALP asters moved apart in relatively linear paths, parallel to the cell long axis, until they reached the ends of the cell. Such excursions could cover over 300 μm and take several hours. Once at the end of the cell, one or both asters could independently undergo rapid rotations of up to 180°, and resume motion in a new direction—often toward the other aster (and fuse to form a normal bipolar spindle; see references 7, 8, and 43). Such astral rotations were never seen once spindle bipolarity was established or in anaphase cells. In more symmetrically-shaped ALP cells, the asters could migrate at obtuse angles relative to one another.

ALP is rare (≤1%) in our primary cultures, and it is impossible to predict before NEB. Therefore, we initiated our observations on ALP cells only after it was clear that the centrosomal MT arrays no longer overlapped (see reference 44). We filmed seven ALP cells for 11 to 34 min each, in which the centrosomes were separating in relatively linear paths. One of these cells and its corresponding analyses are illustrated in Figs. 4 *B* and 5. As during P/PM (see above), the centrosomes in ALP cells exhibited frequent, rapid excursions that could cover 5–6 μm/min (Fig. 4 *B*; *arrowheads* in Fig. 5 *E*); these motions could be directed toward points at any angle from the previous centrosome–centrosome axis (Fig. 4 *B*). As expected, there was no apparent linkage in the behavior of the two centrosomes (Figs. 4 *B* and 5).

We treated the data obtained from ALP cells as detailed for P/PM cells. The results of these analyses are illustrated in Fig. 5 and summarized in Table I. We found no statistically significant difference, over all of the parameters examined, between separating P/PM and ALP centrosomes. This included the average distance moved by each centrosome in 1 min regardless of direction (Table I, line 1; P = 0.47); the frequency at which each centrosome remained "stationary" (Table I, line 2; P = 0.45), exhibited toward (P = 0. 70) or away (P = 0.36) motion; the average vectorial component of away motion per min (Table I, line 3; P = 0.78); the average vectorial component of toward motion per min (Table I,

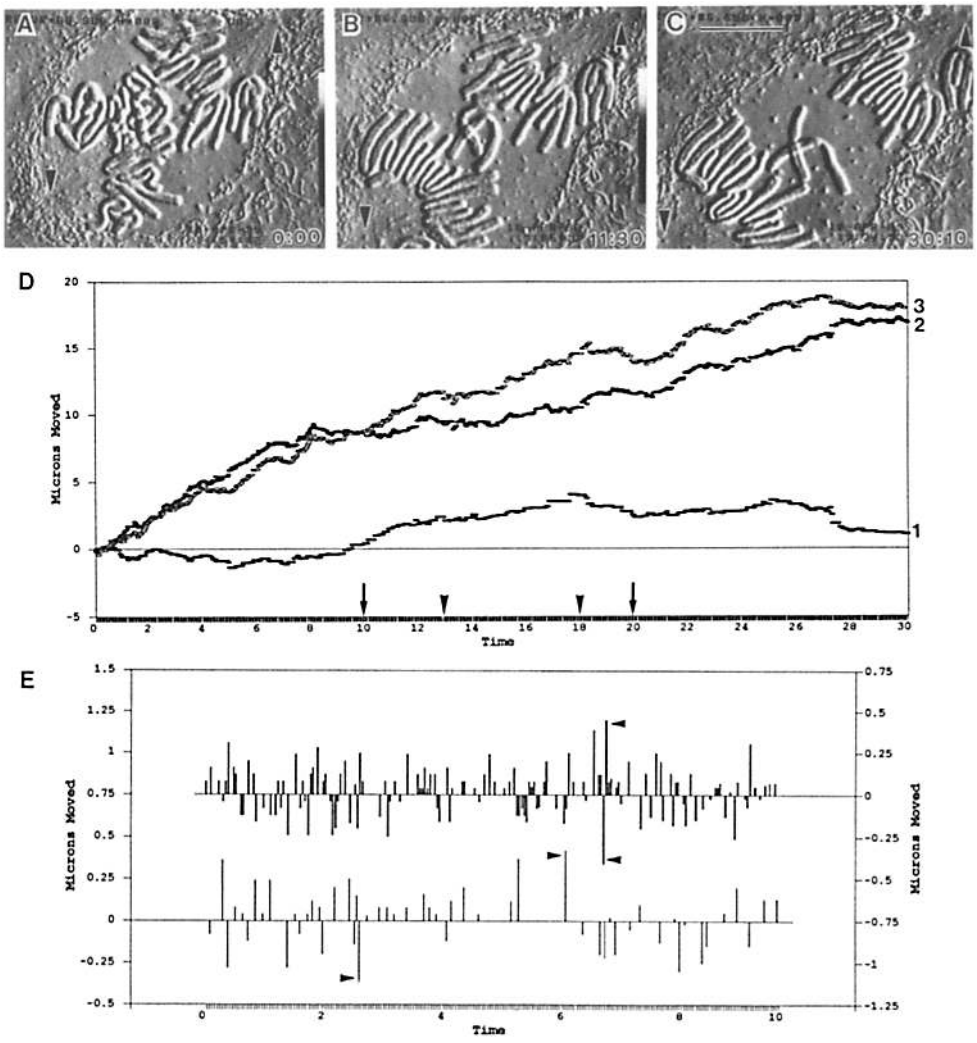

Figure 5. (A–E) Exactly as in Fig. 3 except these centrosomes are in an ALP cell. Arrowheads along the time axis in *D* note that time period covered by the two-dimensional space-time plot in Fig. 4 *B*. Bar (*C*), 20 μm.

line 4; $P = 0.89$); the ratio of total toward/away distance moved (Table I, line 5; $P = 0.15$); and the average contribution of each centrosome to the separation rate over the 10-min window (Table I, line 6; $P = 0.50$) and that of the duration of filming (Table I, line 7; $P = 0.69$).

In summary, over the parameters that we examined, there were no statistically significant differences within and between the data sets of separating centrosomes in P/PM when their MT arrays overlapped, and in ALP when they no longer overlapped.

Anaphase. Once bipolarity was established, the distance between the centrosomes gradually diminished as the spindle became progressively organized and compacted (see reference 52), and the asters shrank in size (Fig. 2, *E–G*). By the onset of anaphase, the spindle was fully compacted, the two asters were at their weakest, and the centrosomes were connected by a dense fusiform-shaped array of spindle MTs (Fig. 2 *H*). Anaphase in NLC's takes 15–20 min, and both anaphase A and B begin with chromatid separation. Because anaphase B continues well after the completion of anaphase A (40), chromosome separation during the last half of anaphase was due exclusively to spindle elongation.

The distribution of MTs during early anaphase resembled that seen in metaphase (cf, Fig. 2, *G* and *H*). By mid-anaphase, the asters were once again conspicuous and the region between the separating centrosomes contained numerous MTs, many of which appeared in each half-spindle as bundles running between the arms of adjacent chromosomes (Fig. 2 *I*). Some of these MTs overlapped with MTs from the other aster. By the end of spindle elongation, the late anaphase cell contained two robust astral MT arrays that were only weakly interconnected by overlapping MTs (Fig. 2 *J*).

We followed centrosome position throughout anaphase in seven cells (e.g., Fig 6). As in the previous stages, each anaphase centrosome spends a considerable amount of the separation period "stationary" (Fig. 6 *E*). Both also exhibited numerous and sometimes rapid (up to 5 μm/min) lateral displacements relative to the previous centrosome–centrosome axis (Fig. 4 *C*, see also *arrowheads* in Fig. 6 *E*). In some instances these motions produced a corresponding motion in the other centrosome (i.e., the spindle was rocking or moving through the cytoplasm), but at other times there was no linkage (Fig. 4 *C*). It is noteworthy that there was no statistically significant difference ($P = 0.71$) between the average distance moved by an anaphase centrosome in 1 min, regardless of direction, and that moved by P/PM and ALP centrosomes (see Table I, line 1).

On average, when compared with P/PM and ALP centrosomes, the frequencies at which anaphase centrosomes re-

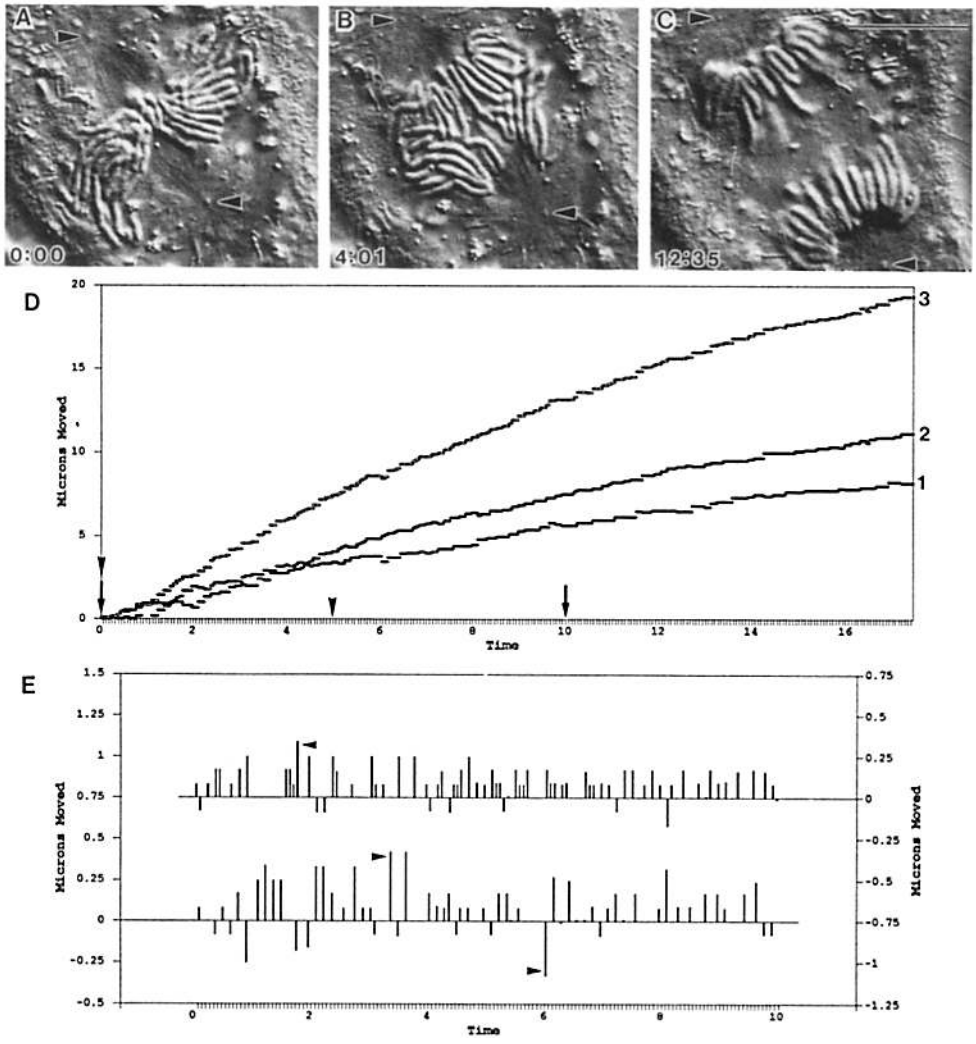

Figure 6. (A–D) Exactly as in Fig. 3 except these centrosomes are in an anaphase cell. Arrowheads along the time axis in (*D*) note that time period covered by the two-dimensional space-time plot in Fig. 4 *C*. Bar (*C*), 20 μm.

mained "stationary" or exhibited away motion (Fig. 6 *E*) were not different (Table I, line 2; $P = 0.70$ and 0.08, respectively). In addition, the rate of away motion was not different than that of centrosomes in P/PM and ALP cells (Table I, line 3; $P = 0.48$). However, when compared with P/PM and ALP, anaphase centrosomes spent significantly less time moving toward the other centrosome (Table I, line 2; $P = 0.02$), and the average rate of this movement was significantly less (Table I, line 4; $P \leq 0.0001$).

A comparison of direct-distance plots revealed that, as a rule, anaphase centrosomes separated in a smoother and more linear fashion than in P/PM or ALP (cf Figs. 3 *D*, 5 *D*, and 6 *D*). The average contribution of each centrosome to the separation rate was 0.51 ± 0.07 μm/min (Table I, line 7), which was significantly faster ($P = 0.01$) than that exhibited by P/PM or ALP centrosomes. The same was found when comparing data during the 10-min windows in which the most separation occurred (Table I, line 6). Finally, the ratio of toward-versus-away distance moved by anaphase centrosomes was significantly less (Table I, line 5; $P = 0.0007$) than that exhibited by P/PM or ALP centrosomes.

In summary, when compared with separating P/PM and ALP centrosomes, anaphase centrosomes moved away from their partners, on average, with the same frequency and rate but exhibited a significantly lower frequency and rate of toward motion. When combined, these characteristics describe a significantly faster rate of centrosome separation during anaphase than during prophase or ALP.

Discussion

Our results are relevant to the mechanism of centrosome separation in vertebrate cells during both spindle formation and anaphase spindle elongation.

Spindle Formation

Our knowledge of centrosome separation in vertebrates is derived primarily from work on anaphase. With the exception of drug (e.g., 11, 52) and structural (e.g., 32, 39, 45) studies implicating MTs in the process, there are little additional data on how the duplicated centrosomes separate at the onset of mitosis. In our study we took advantage of the fact that separating asters move apart until they reach the periphery of the cell if they do not become tethered via bipolar-oriented chromosomes. The experimental aspect of this behavior is that when the asters do not become tethered in an appropriately elongated cell, they separate to the point where their MT arrays no longer overlap but then continue to separate after that point (to form an ALP mitotic figure;

for human carcinoma see reference 56; for PtK see references 10 and 19; for newts see references 8 and 40).

Our major finding is that there are no statistically significant differences in the behavioral characteristics of separating centrosomes in P/PM cells regardless of whether or not their MT arrays overlap. This includes, e.g., the average total displacement, the average rate of vectorial motion directed toward and away from the other centrosome, the frequency of each type of motion, and the average rate contributed by each centrosome to the separation process. From our data we conclude that the force for centrosome separation during spindle formation in vertebrates is produced independently by each aster.

This conclusion is inconsistent with the popular "pushing" hypothesis in which the centrosomes "propel themselves to the opposite mitotic poles by pushing against each other through the spindle which they generate" (12). Mechanistically, this model envisions that interacting MTs derived from opposing centrosomes, elongate and slide past one another through the action of MT plus-end directed motor proteins (reviewed in references 14 and 30). It is supported by two principal lines of evidence both of which are circumstantial. First, centrosome separation in cells recovering from MT-disrupting drugs is coincident with the growth of MTs (e.g., 11, 23); second, the two spindle poles in many organisms (e.g., yeast, algae, some fungi) are linked during separation by prominent, highly-ordered interconnected MT arrays of opposite polarity (reviewed in references 14 and 18). However, the former finding reveals only that MTs are somehow involved in the separation process, while the applicability of the latter to vertebrates has never been convincingly demonstrated. Indeed, unlike diatoms and yeast, the two separating centrosomes in vertebrate P/PM cells are at best weakly inter-connected by MTs (Fig. 2 *B*; see also references 7, 32, 38, and 45).

Our data validate for the astral mitosis of vertebrates the original model for centrosome separation proposed in the 1880s by Van Beneden and Boveri (see refence 56, pp 178–179). This hypothesis envisions the asters to be independent, autonomous units, that pull themselves apart. That asters possess intrinsic MT-dependent properties enabling them to move independently through the cytoplasm has been clearly demonstrated on numerous occasions. For example, upon fertilization in most animals, the sperm aster, with its associated paternal pronucleus, migrates from its cortical site of entry through the egg cytoplasm to the female pronucleus in the absence of a second aster (e.g., 16, 48). Similarly, when single asters are detached by micromanipulation from the sand dollar (21) or sea urchin (reviewed in reference 49) spindle, they tend to migrate away from the spindle region. Finally, we and others (6, 7) have shown that the mitotic asters in ALP cells undergo independent and extensive migrations within the cell.

We found that NLC centrosomes undergo an average displacement of $\sim$2 μm/min during all separation stages (Table I, line 1). However, during P/PM and ALP each exhibits independently an average vectorial rate of motion away from the other of only 0.30–40 μm/min. Thus, much of the centrosomes' motion is directed toward other points within the cell. As confirmed by our two-dimensional space-time plots, they do not separate in a straight line. Moreover, during 45–55% of the separation period each centrosome is either stationary or moving in a direction that does not increase its distance from the other centrosome. It exhibits motion directed away from the other centrosome 25–35% of the time, and motion directed toward the other centrosome 15–20% of the time. It is noteworthy that the average rate of away motion is the same during both P/PM and ALP (when there is no MT overlap), and that it is greater than the toward motion vector.

Our data clearly reveal that each separating centrosome undergoes frequent and significant motions toward random points within the cell, and that only some of these motions contribute to separation. How is the frequency and magnitude bias for forward motion established, given our conclusion that centrosomes are not pushed apart via MT-MT interactions between opposing asters? The most likely explanation is that separating asters have an intrinsic polarity that, over time, favors net displacement in a particular direction. In this respect it is important that asters in ALP cells always move "in a direction opposite the direction of deformation of the aster caused by" associated monooriented chromosomes (7; our observations), and are never seen to change their direction of migration without first rotating toward the new direction (our observations; see also reference 8). It is currently unclear how this polarity is established, but it likely involves aster symmetry (see below). In contrast to polarity, which defines the part of the aster that leads in motion, the migratory direction appears to depend on cell shape: in symmetrical cells the asters can move away from each other at various angles relative to the long axis of the nucleus (e.g., 6, 43) whereas in rectangular cells motion is largely restricted to a direction parallel to the cell long axis.

The direction of astral motion is always along or toward the best developed (longest) arrays of MTs (e.g., 7, 16, 20), and asters in NLCs (7) and sand-dollar eggs (16) stop moving when they become symmetrical, i.e., when all the MTs are of similar length. These findings led to the hypothesis that "asters move by unbalanced traction forces that are generated along astral rays and are proportional to their length" (16). One possible mechanism for producing such a force/length relationship is to randomly distribute anchored minus-end-directed MT motors on the ventral surface of the plasma membrane. Under this condition short MTs making limited or no contact with the membrane would not participate in force generation/transmission. By contrast, those MTs making extensive (lateral) contact with the membrane would participate, and the longer the MT the greater the potential pulling force it can exert on the centrosome. Subtle or radical directional changes of moving asters observed in our study would be a manifestation of rapid changes in the length and distribution of MTs predicted from MT dynamic instability (reviewed in reference 25).

How is the polarized motion of asters explained by such a force-producing mechanism? At least during pronuclear migration in zygotes and ALP, the asters possess tightly attached pronuclei or chromosomes that impart asymmetry by blocking or restricting the growth of MTs through the structure. Motion is impeded in the direction of the blockage because fewer MTs can extend through the blocking structures to contact the membrane. Because there are more force-producing MTs on the side of the aster opposite the blockage the aster will move over time in that direction. The bias for aster separation during P/PM may similarly involve aster asymmetry (see Fig. 2 *B*; also reference 39) produced, e.g., by

the unequal distribution of MT-nucleating material around the diplosome (see reference 41).

Anaphase Spindle Elongation

It has been argued that anaphase B centrosome separation in vertebrates, like the diatom (e.g., 14) and other highly-ordered anaphase spindles (e.g., yeast; 51), is mediated by a pushing mechanism (e.g., 14, 15, 22, 27, 29, 30). However, as during P/PM much of this argument is based on data obtained from drug (e.g., 5, 35) and structural (e.g., 13, 28) studies that are equally consistent with the pulling hypothesis. Likewise, relevant data obtained by more experimentally-based approaches (e.g., FRAP and in vitro models; see references 37 and 46), which has also been forcefully interpreted to support the pushing model, is still circumstantial and consistent with other interpretations (e.g., see references 26 and 47).

To date, the best evidence in support of a pushing mechanism for centrosome separation during anaphase in vertebrates is that of Nislow et al. (34; see also reference 33). These investigators cloned a kinesin-like protein that localizes, by IMF criteria, to the midzone of mammalian anaphase cells. In vitro, this protein binds tightly to MTs and promotes bundling of anti-parallel MTs, suggesting that it plays a role in holding "the antiparallel microtubules of the two interdigitating half spindles together during anaphase" (33). More important to the mechanism of centrosome separation is that this protein also appears in some assays to move MTs relative to one another in a plus end direction (34). Unfortunately, antibodies to this protein do not inhibit spindle elongation when microinjected into mitotic cells (33).

We found that anaphase centrosomes separated at significantly faster rates than those in P/PM or ALP cells. However, we also found that the average vectorial rate of the away motion was not statistically different from that of P/PM and ALP cells. The explanation for this apparent rate dichotomy is evident from our data: when compared with P/PM and ALP, an anaphase centrosome undergoes significantly fewer motions at substantially reduced rates toward the other centrosome. Thus, unlike P/PM and ALP, where over time much of the vectorial away motion is canceled by an opposite toward motion, a greater amount of the vectorial away motion exhibited by an anaphase centrosome actually contributes to the separation process.

We also found that anaphase centrosomes exhibit the same average (Table I, line 1) and maximum ($\sim$5–6 μm/min) rates of displacement as found for P/PM and ALP centrosomes and, like in the earlier stages, these displacements could be directed towards any point within the cell. These findings, together with the fact that the average vectorial away motion in anaphase is not different from that in P/PM and ALP cells (Table I, line 3), lead us to conclude that centrosome motion during all of these stages is produced by the same force-producing mechanism which is intrinsic to each aster. Our data also clearly demonstrate that, unlike the forming spindles of P/PM, the anaphase spindle impedes the motion of centrosomes toward one another. The most straightforward interpretation of these results is that the overlapping interzonal MT arrays that indirectly connect the centrosomes during anaphase in vertebrates act as a ratchet that allows the centrosomes to separate while impeding motion toward one another. Such a ratchet mechanism may be mediated by proteins that bind to antiparallel MTs such as that recently described by Nislow et al. (34). A linkage of overlapping, antiparallel spindle MTs during anaphase would ensure centrosome separation by inhibiting astral rotation and motion toward one another. Regardless, the interaction of antiparallel astral MTs within the spindle does not prevent the metaphase/anaphase centrosome from attempting to migrate within the cell, as evidenced by the constant rocking and bending motions exhibited by the spindle—clearly due to forces associated with the aster and not the central spindle (see also reference 2).

Our conclusion that centrosome separation during anaphase results from pulling forces associated with each aster is not without precedent. A similar conclusion was reached by Aist and Berns (1; see also reference 3) and Kronebusch and Borisy (26). The former severed the anaphase spindle in *Fusarium solani* (fungi) with a UV laser, whereas the latter used mechanical means to cut the anaphase spindle in PtK cells. In both experiments the centrosomes separated at an enhanced rate, leading to the conclusion that the interzonal MTs limited the rate of separation and did not provide the motive force. Evidence that the aster is involved in spindle elongation also comes from Hiramoto et al. (20; see also reference 21), who irradiated selected regions of Colcemid-treated sand dollar eggs with 365-nm light to photochemically inactivate the Colcemid within that region. When the centrosomes and chromosomes were included in the irradiation area a spindle was rapidly assembled that underwent a normal anaphase. By contrast, when only that area between the centrosomes (i.e., the chromosomes) was irradiated, a spindle assembled that moved chromosomes poleward during anaphase, but failed to elongate.

This paper is dedicated to Dr. A. S. Bajer who taught C. L. Rieder that the cell is always "talking"—the secret is to learn its language. We would like to thank Drs. S. Bowser, J. Ault, C. A. Mannella, C. Jensen, E. D. Salmon, and S. P. Alexander for stimulating discussions and comments; Dr. A. Leith for his assistance with Eq. 1 and computer programming; and Ms. S. Nowogrodzki for editorial assistance and artwork.

This work was supported in part by National Institutes of Health General Medical Sciences grant R01-40198 (to C. L. Rieder), and by RR 01219 awarded by the Center for Research Resources, Department of Health and Human Resources/Public Health Service, to support the Wadsworth Center's Biological Microscopy and Image Reconstruction Facility as a National Biotechnological Resource.

Received for publication 2 March 1993 and in revised form 7 April 1993.

References

1. Aist, J. R., and M. W. Berns. 1981. Mechanics of chromosome separation during mitosis in *Fusarium* (fungi imperfecti): new evidence from ultrastructural and laser microbeam experiments. *J. Cell Biol.* 91:446–458.
2. Aist, J. R., C. J. Bayles, W. Tao, and M. W. Berns. 1991. Direct experimental evidence for the existence, structural basis and function of astral forces during anaphase B in vivo. *J. Cell Sci.* 100:279–288.
3. Aist, J. R., H. Liang, and M. W. Berns. 1993. Astral and spindle forces in mitotic PtK_2 cells. A laser microbeam study. *J. Cell Sci.* 104: 1207–1216.
4. Alexander, S. P., and C. L. Rieder. 1991. Chromosome motion during attachment to the vertebrate spindle: initial saltatory-like behavior of chromosomes and quantitative analysis of force production by nascent kinetochore fibers. *J. Cell Biol.* 113:805–815.
5. Amin-Hanjani, S., and P. Wadsworth. 1991. Inhibition of spindle elongation by taxol. *Cell Motil. Cytoskel.* 20:136–144.
6. Aubin, J. E., M. Osborn, and K. Weber. 1980. Variations in the distribution and migration of centriole duplexes in mitotic PtK_2 cells studied by immunofluorescence microscopy. *J. Cell Sci.* 43:177–194.
7. Bajer, A. S., and J. Mole-Bajer. 1981. Asters, poles, and transport properties within spindle-like microtubule arrays. *Cold Spring Harbor Symp.*

Quant. Biol. 46:263–283.
8. Bajer, A. S. 1982. Functional autonomy of monopolar spindle and evidence for oscillatory movement in mitosis. *J. Cell Biol.* 93:33–48.
9. Bre, M.-H., T. E. Kreis, and E. Karsenti. 1987. Control of microtubule nucleation and stability in Madin-Darby canine kidney cells: the occurrence of noncentrosomal, stable detyrosinated microtubules. *J. Cell Biol.* 105:1283–1296.
10. Brenner, S., A. Branch, S. Meredith, and M. W. Berns. 1977. The absence of centrioles from spindle poles of rat kangaroo (PtK2) cells undergoing meiotic-like reduction division in vitro. *J. Cell Biol.* 72:368–379.
11. Brinkley, B. R., E. Stubblefield, and T. C. Hsu. 1967. The effects of Colcemid inhibition and reversal on the fine structure of the mitotic apparatus in Chinese hamster cells in vitro. *J. Ultrastruct. Res.* 19:1–18.
12. Brinkley, B. R., and E. Stubblefield. 1970. Ultrastructure and interaction of the kinetochore and centriole in mitosis and meiosis. *In* Advances in Cell Biology. D. M. Prescott, L. Goldstein, and E. McConkey, editors. 1:119–185.
13. Brinkley, B. R., and J. Cartwright. 1971. Ultrastructural analysis of mitotic spindle elongation in mammalian cells in vitro. Direct microtubule counts. *J. Cell Biol.* 50:416–431.
14. Cande, W. Z., and C. J. Hogan. 1989. The mechanism of anaphase spindle elongation. *BioEssays* 11:5–9.
15. Goldstein, L. S. B. 1992. Functional redundancy in mitotic force generation. *J. Cell Biol.* 120:1–3.
16. Hamaguchi, M. S., and Y. Hiramoto. 1986. Analysis of the role of astral rays in pronuclear migration in sand dollar eggs by the Colcemid-UV method. *Dev. Growth Differ.* 28:143–156.
17. Hayden, J., S. S. Bowser, and C. L. Rieder. 1990. Kinetochores capture astral microtubules during chromosome attachment to the mitotic spindle: direct visualization in live newt lung cells. *J. Cell Biol.* 111:1039–1045.
18. Heath, I. B. 1979. Variant mitoses in lower eukaryotes: indicators of the evolution of mitosis. *Intl. Rev. Cytol.* 64:1–80.
19. Heneen, W. K. 1970. In situ analysis of normal and abnormal patterns of the mitotic apparatus in cultured rat-kangaroo cells. *Chromosoma.* 29: 88–117.
20. Hiramoto, Y., Y. Hamaguchi, M. S. Hamaguchi, and Y. Nakano. 1986. Roles of microtubules in pronuclear migration and spindle elongation in sand dollar eggs. *In* Cell Motility: Mechanisms and Regulation. H. Ishikawa, S. Hatano, and H. Sato, editors. Alan R. Liss, Inc., NY. 349–356.
21. Hiramoto, Y., and Y. Nakano. 1988. Micromanipulation studies of the mitotic apparatus in sand dollar eggs. *Cell Motil. Cytoskel.* 10:172–184.
22. Hogan, C. J., and W. Z. Cande. 1990. Antiparallel microtubule interactions: spindle formation and anaphase B. *Cell Motil. Cytoskel.* 16: 99–103.
23. Hyman, A. A., and J. G. White. 1987. Determination of cell division axes in the early embryogenesis of *Caenorhabditis elegans*. *J. Cell Biol.* 105:2123–2135.
24. Joshi, H. C., M. J. Palacios, L. McNamara, and C. W. Cleveland. 1992. Gamma tubulin is a centrosomal protein required for cell cycle-dependent microtubule nucleation. *Nature (Lond.).* 356:80–83.
25. Kirschner, M. W., and T. J. Mitchison. 1986. Beyond self-assembly: from microtubules to morphogenesis. *Cell.* 45:329–342.
26. Kronebusch, P. J., and G. G. Borisy. 1982. Mechanisms of anaphase B movement. *In* Biological Function of MTs and Related Structures. H. Sakai, H. Mohari, and G. G. Borisy, editors. Academic Press, New York. 233–245.
27. Mazia, D. 1987. The chromosome cycle and the centrosome cycle in the mitotic cycle. *Intl. Rev. Cytol.* 100:49–92.
28. McIntosh, J. R., and S. C. Landis. 1971. The distribution of spindle microtubules during mitotis in cultured human cells. *J. Cell Biol.* 49:468–497.
29. McIntosh, J. R., and G. E. Hering. 1991. Spindle fiber action and chromosome motion. *Annu. Rev. Cell Biol.* 7:403–426.
30. McIntosh, J. R., and C. N. Pfarr. 1991. Mitotic Motors. *J. Cell Biol.* 115:577–585.
31. Mitchison, T. J. 1989. Mitosis: basic concepts. *Curr. Opin. Cell Biol.* 1:67–74.
32. Mole-Bajer, J. 1975. The role of centrioles in the development of the astral spindle (newt). *Cytobios.* 13:117–140.
33. Nislow, C., C. Sellitto, R. Kuriyama, and J. R. McIntosh. 1990. A monoclonal antibody to a mitotic microtubule-associated protein blocks mitotic progression. *J. Cell Biol.* 111:511–522.
34. Nislow, C., V. Lombillo, R. Kuriyama, and J. R. McIntosh. 1992. A plus-end directed motor enzyme that moves antiparallel microtubules *in vitro* localizes to the interzone of mitotic spindles. *Nature (Lond.).* 359: 543–547.
35. Oppenheim, D. S., B. T. Hauschka, and J. R. McIntosh. 1973. Anaphase motions in dilute colchicine. Evidence of two phases in chromosome segregation. *Exp. Cell Res.* 79:95–105.
36. Paintrand, M., M. Moudjou, H. DeLacroix, and M. Bornens. 1992. Centrosome organization and centriole architecture: their sensitivity to divalent cations. *J. Struct. Biol.* 108:107–128.
37. Palazzo, R. E., D. A. Lutz, and L. I. Rebhun. 1991. Reactivation of isolated mitotic apparatus: metaphase versus anaphase spindles. *Cell Motil. Cytoskeleton* 18:304–318.
38. Rattner, J. B., and M. W. Berns. 1976*a*. Centriole behavior in early mitosis of rat kangaroo cells (PtK_2). *Chromosoma.* 54:387–395.
39. Rattner, J. B., and M. W. Berns. 1976*b*. Distribution of microtubules during centriole separation in rat kangaroo (*Potorous*) cells. *Cytobios.* 15:37–43.
40. Rieder, C. L. 1977. An in vitro light and electron microscopic study of anaphase chromosome movements in normal and temperature elevated *Taricha* lung cells. PhD Thesis, University of Oregon, Eugene, OR.
41. Rieder, C. L., and G. G. Borisy. 1982. The centrosome cycle in PtK_2 cells: asymmetric distribution and structural changes in the pericentriolar material. *Biol. Cell.* 44:117–132.
42. Rieder, C. L. 1990. Formation of the astral mitotic spindle: ultrastructural basis for the centrosome-kinetochore interaction. *Electron Microsc. Rev.* 3:269–300.
43. Rieder, C. L., and R. Hard. 1990. Newt lung epithelial cells: Cultivation, use and advantages for biomedical research. *Intl. Rev. Cytol.* 122: 153–220.
44. Rieder, C. L., and S. P. Alexander. 1990. Kinetochores are transported poleward along a single astral microtubule during chromosome attachment to the spindle in newt lung cells. *J. Cell Biol.* 110:81–96.
45. Roos, U.-P. 1973. Light and electron microscopy of rat kangaroo cells in mitosis. I. Formation and breakdown of the mitotic apparatus. *Chromosoma.* 40:43–82.
46. Saxton, W. M., and J. R. McIntosh. 1987. Interzone microtubule behavior in late anaphase and telophase spindles. *J. Cell Biol.* 105:875–886.
47. Shelden, E., and P. Wadsworth. 1990. Interzonal microtubules are dynamic during spindle elongation. *J. Cell Sci.* 97:273–281.
48. Sluder, G., and C. L. Rieder. 1985. Experimental separation of pronuclei in fertilized sea urchin eggs. Chromosomes do not organize a spindle in the absence of centrosomes. *J. Cell Biol.* 100:897–903.
49. Sluder, G. 1990. Experimental analysis of centrosome reproduction in echinoderm eggs. *Adv. Cell Biol.* 3:221–250.
50. Snyder, J. A., R. J. Golub, and S. P. Berg. 1984. Sucrose-induced spindle elongation in mitotic PtK-1 cells. *Eur. J. Cell Biol.* 35:62–69.
51. Sullivan, D. S., and T. C. Huffaker. 1992. Astral microtubules are not required for anaphase B in *Saccharomyces cerevisiae*. *J. Cell Biol.* 119:379–388.
52. Taylor, E. W. 1959. Dynamics of spindle formation and its inhibition by chemicals. *J. Biophys. Biochem. Cytol.* 6:193–196.
53. Vandre, D. D., F. M. Davis, P. N. Rao, and G. G. Borisy. 1984. Phosphoproteins are components of mitotic microtubule organizing centers. *Proc. Natl. Acad. Sci. USA.* 81:4439–4443.
54. Vandre, D. D., and G. G. Borisy. 1989. The centrosome cycle in animal cells. In Mitosis: Molecules and Mechanisms. J. S. Hyams and B. R. Brinkley, editors. Academic Press, NY. 39–76.
55. Verde, F., J.-C. Labbe, M. Doree, and E. Karsenti. 1990. Regulation of microtubule dynamics by *cdc 2* protein kinase in cell-free extracts of *Xenopus* eggs. *Nature (Lond.).* 343:233–238.
56. Wilson, E. B. 1925. The Cell in Development and Heredity. 3rd Edition, MacMillan Co., NY. 1232.